Study on Transmission Characteristics of a Hybrid Triangle Wedge Surface Plasmonic Polaritons Waveguide with Subwavelength Mode Confinement

Zhao Hai Song Qing Sun Haili Zhang Guanmao

Institute of Modern Communication Technology, School of Information Science and Engineering, Lanzhou University, Lanzhou, Gansu 730000, *China*

Abstract A novel metal-dielectric-metal (MDM) waveguide based on the hybrid surface plasmonic polaritons (HSPPs) is proposed and numerically analyzed. This waveguide consists of two metal triangle wedge is placed on both sides of dielectric nanowires. Analytical and numerical calculations based on the finite element method (FEM) are carried out at the telecommunication wavelength $\lambda = 1.55\ \mu m$. The numerical results show that it can confine light in the ultra-deep-subwavelength region with long propagation distance relative to the distance in the MDM waveguide without metal triangle. Detailed study of this structure reveals that these advantages originate from the tip enhancement of the triangle semiconductor waveguide. At 120°, its propagation distance increase 18% and mode area decrease 65%. So various applications will benefit from the hybrid plasmonic polariton waveguides, such as the laser, coupler and photonic integrated circuits.

Key words integrated optics; photonic integrated circuits; surface plasmonic polariton waveguides; finite element method; 1 dB angle wide

OCIS codes 130.3120; 130.3990; 130.5460

一种具有亚波长模式限制的三角楔形混合表面等离子激元波导传输特性研究

赵 海 宋 卿 孙海丽 张冠茂

兰州大学信息科学与工程学院现代通信技术研究所, 甘肃 兰州 730000

摘要 提出并数值分析了基于混合表面等离子激元(HSPPs)的新型金属-介质-金属(MDM)波导,这种波导是由介质纳米线两侧的金属三角楔形结构构成。在通信波长 1.55 μm 情形下,基于有限元方法(FEM)进行了分析和数值计算,计算结果表明光波能够被限制在超深亚波长区域,并且相比于没有三角楔形的波导结构具有更长的传播长度。更进一步的研究显示出该三角形半导体波导具有尖端增强效应,在三角楔形的顶角为120°时,其传播长度提高了18%且模式面积减小为原来的65%,因此这种混合表面等离子激元波导可应用于激光器、耦合器以及光子集成电路的设计中。

关键词 集成光学; 光子集成电路; 表面等离子激元波导; 有限元法; 1 dB角宽

中图分类号 0436 **文献标识码** A

doi: 10.3788/LOP52.091301

1 Introduction

For next-generation on-chip technology, the high-density integrated photonic circuits are attracting interest[1]. Surface plasmon polaritons (SPPs)[2-3] which are electromagnetic waves coupled to collective

收稿日期: 2015-02-03; **收到修改稿日期**: 2015-04-23; **网络出版日期**: 2015-08-14

基金项目: 中央高校基本科研业务费专项资金资助(兰州大学)(lzujbky-2012-40,lzujbky-2015-K7)

作者简介: 赵 海(1988—),男,硕士研究生,主要从事表面等离子激元波导技术方面的研究。E-mail: zhaohai12345678@163.com

导师简介: 张冠茂(1973—),男,副教授,博士,主要从事光通信、光传感、微纳光子晶体以及光域表面等离子激元共振方面的研究。E-mail: zhanggm@lzu.edu.cn(通信联系人)

electron oscillation and propagating along the interface between a metal and a dielectric is drawing more and more attentions due to it offers the opportunity to confine and guide light beyond the diffraction limit[4]. Hu Qing et al[5] provides a new and promising approach for realizing spatiotemporal-sensitive spectral splitting and optical signal processing on nanoscales. Wei Wei et al[6] theoretically investigated the plasmonic waveguiding properties of the gap plasmon mode between two adjacent silver nanowires with a substrate. Ditlbacher H et al[7] discussed the experimental realization of efficient optical element built up from metal nanostructures to manipulate surface plasmon polaritons propagating along a silver/polymer interface. In recent years, many SPP waveguides such as dielectric-metal-dielectric (DMD)[8], V-groove channel[9-10], metal wedge[11], dielectric-loaded surface plasmon polariton waveguides (DLSPPW)[12-14]. However, there is a trade-off relation between the propagation distance and the field confinement for these surface plasmonic polariton waveguides. But metal-dielectric-metal (MDM) structures not only have small propagation loss but also can provide subwavelength mode confinement[15]. Such ultra-deep-subwavelength mode confinement could be used for various applications, such as: plasmonic[16]、coupler[17]、sensor[18]、nanolasers[19] and nanoparticle trapping by optical forces[20].

A novel MDM hybrid surface plasmonic polaritons (HSPP) waveguide consisting of two metal cladding with a triangle wedge symmetrically located on both sides of a dielectric nanowire embedded in SiO_2 cladding above a low-index dielectric substrate is proposed. According to previous research, the symmetry structure has better propagation distance than the asymmetry one at the same situation. Meanwhile, this SPP waveguide with the triangle wedge is not only low propagation loss but also stronger mode confinement than without it. Besides, considering the practical fabricated error, the arc of the tip on the triangle wedge is analyzed. The results show that the triangle wedge waveguide is very potential for ultra-strong light-matter interactions in the future.

2 Theory analysis and waveguide structures

Figure 1 draws the proposed hybrid triangle wedge surface plasmonic polaritons (HTWSPPs) waveguide, which consists of a Si nanowire embedded in a low permittivity SiO_2 cladding and its two sides are placed two identical silver layer with a triangle wedge which is near a small gap g in the Si nanowire. The silver layer loaded low-index glass substrate with SiO_2 cladding in its other side. The diameter of the nanowire is D and the thickness of the silver film is t. The silver wedge has tip angle of θ and the height of h. In the numerical simulations, the wavelength is selected as $\lambda = 1.55\ \mu m$ and the corresponding permittivities of SiO_2 is assumed to be $\varepsilon_{SiO_2} = 2.25$ respectively and the index of the low-index Cytop substrate is $n_s = 1.34$ [21]. At $\lambda = 1.55\ \mu m$, due to the extinction coefficient of Si is zero and $n_{Si} = 3.48$, so the permittivity of Si is $\varepsilon_{Si} = 12.25$ [22-23]. By the Drude model, the permittivity of silver is defined as $\varepsilon_{Ag} = -129 + 3.3i$ at $\lambda = 1.55\ \mu m$ [24].

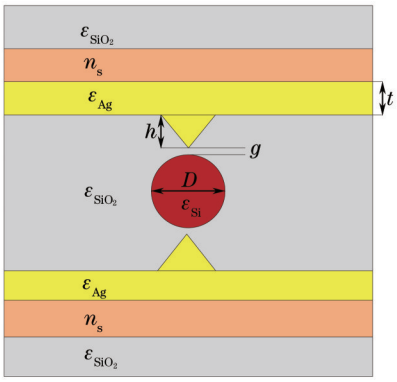

Fig.1 Cross section of the proposed HTWSPPs waveguide

3 Properties of waveguide

The model transmission characteristics have been calculated by the finite element method (FEM), such as propagation distance, mode area, the figure of merits (FOM), coupling length. Here the propagation distance is calculated as $L_p = \lambda/[4\pi\ \mathrm{Im}(n_{\mathrm{eff}})]$ [25], where the Im (n_{eff}) is the imaginary part of the mode effective refractive index n_{eff} in the simulation results. The normalized mode area is expressed by the equation $A = A_{\mathrm{eff}}/A_0$, where $A_0 = \lambda^2/4$ is the diffraction-limited mode area and the effective mode area A_{eff} is defined as[26]

$$A_{\mathrm{eff}} = \frac{W_m}{\max[W(x,y)]} = \frac{\iint_\infty W(x,y)\mathrm{d}x\mathrm{d}y}{\max[W(x,y)]}, \tag{1}$$

where $W(x,y)$ is the total electromagnetic (EM) energy density

$$W(x,y) = \frac{1}{2}\mathrm{Re}\left\{\frac{\mathrm{d}[\omega\varepsilon(x,y)]}{\mathrm{d}\omega}\left|E(x,y)\right|^2 + \mu_0\left|H(x,y)\right|^2\right\}, \tag{2}$$

where $\left|E(x,y)\right|^2$ and $\left|H(x,y)\right|^2$ are the electric and magnetic field respectively.

3.1 Effective refractive index

First, the influence of the tip angle θ of the triangle nanowedges with the gap g on the model properties of the waveguide is discussed. In the simulation, the parameters used here are t=100 nm, D=100 nm and h=50 nm. Figure 2 shows the dependence of the real and imaginary part of the mode effective refractive index n_{eff} with the gap g. It firstly decreases and then increases slowly along the increase of the tip angle θ. The mode effective index increases on account of a majority of the electromagnetic field into the high index Si nanowire.

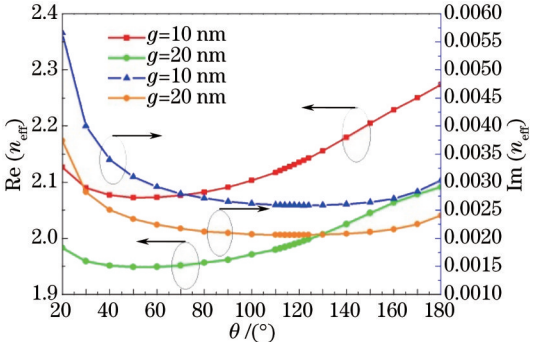

Fig.2 Real part and imaginary part of the mode effective refractive index n_{eff}

3.2 Propagation distance and mode confinement

As shown in Figure 3(a) and (b), with the increase of the tip angle θ, the normalized mode area increases monotonically and then quickly after 120°, it is found that the normalized mode area of the hybrid mode is directly related to the interface area between metal and the low-index dielectric cladding, the interface area

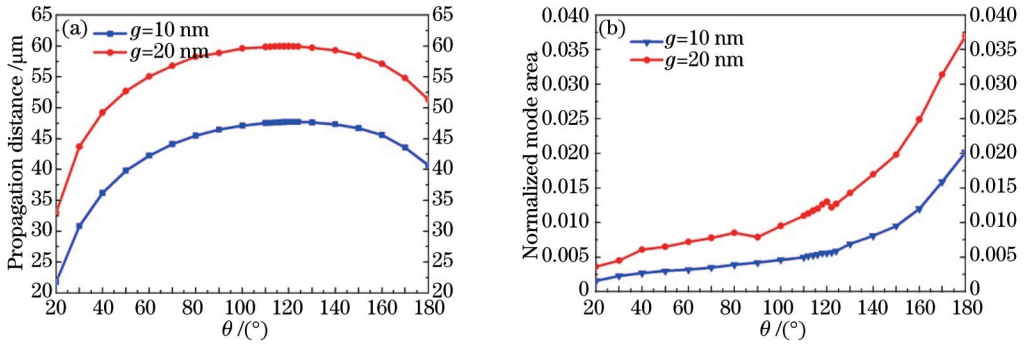

Fig.3 Dependence of the transmission characteristics of the provided waveguide on the θ in different g (g=10 nm, g=20 nm). (a) Propagation distance; (b) normalized mode area

increase resulting in raise of the mode area with the increase of the angle θ. Meanwhile, the propagation distance is shown that it increases at first and then decreases as the tip angle θ increases from 20° to 180°, and it also reachs the maximum value at certain tip angle θ (i.e, θ = 120°).

In this structure, at θ = 180°, it is a special point in which the metal layer has not the triangle wedge. From Figure 3(a) and (b), it is obvious that the waveguide with triangle wedge shows the better confinement ability and the propagation distance of these waveguides are improved from 60° to 170° compared to those ones without it. At 120°, its propagation distance increases 18% and the mode area decreases 65% than the structure without it. Therefore, the proposed waveguide shows great advantages of better confinement and lower propagation loss[27].

The propagation distance could be further increased by increasing the gap g between the triangle wedge and nanowire at the expense of weaker mode confinement. The normalized electromagnetic energy density distributions of three points a (g=10 nm, θ =120°), b (g=20 nm, θ =120°) and c (g=20 nm, θ = 160°) are plotted in Figure 4 (a), (b) and (c). From figure 4, it is clear that the electromagnetic field is tightly confined around the nanowedges tip regions. It shows that the increase of the gap distance will decrease the mode confinement with the same tip angle. Figure 4(b) and (c) show also that a greater proportion of the electric field spreads laterally along the metal wedge resulting in a larger portion of power distributed in the metal region giving rise to a larger metallic dissipation in the same gap with the increase of tip angle θ, the reason is that the large degree always is the large mode area.

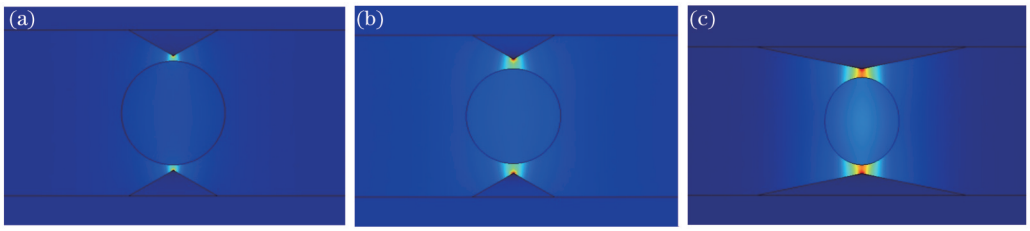

Fig.4 Normalized EM energy density distributions of different points.
(a) g=10 nm, θ =120°; (b) g=20 nm, θ =120°; (c) g=20 nm, θ =160°

3.3 Figure of merits

For evaluating systematically the advantage of the waveguide, the FOM is defined by[28]

$$V_{\mathrm{FOM}} = \frac{L_{\mathrm{p}}}{2}\sqrt{\frac{\pi}{A}}, \tag{3}$$

Where L_{p} is the propagation distance and A is the normalized mode area. This parameter shows the trade-off relation between propagation distance and normalized mode area. From figure 5, when the tip angle is less than 40°, the red solid curve (g=20 nm) is superior than the blue solid curve (g=10 nm), this result is converse larger than 40° and the FOM have the maximum value around 120°. So it shows that the longest propagation distance for the best confinement is at the same degree or it has the best confinement for the

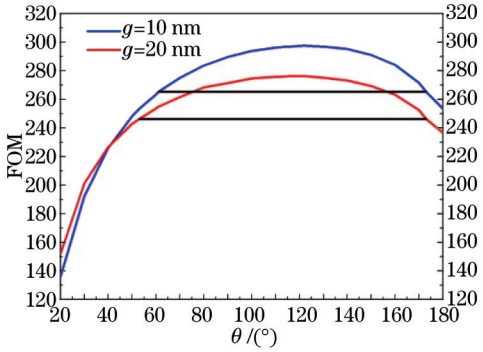

Fig.5 Relation between the FOM and the tip angle θ for different g, the two horizontal lines are 1 dB angle wide for different g (g=10 nm, g=20 nm)

same propagation loss. Considering the flexibility of the structure, it is allowed that fluctuation of the tip angle around 120°. In the actual process, the 1 dB of wide angle is defined as its variation from the maximum to it that the FOM is smaller than 1 dB in the angle range, as shown in Figure 5 (i.e, g=10 nm, from 47° to 172°, g=20 nm, from 60° to 172°). Above it, the waveguide may have the better FOM over a wide angle range.

3.4 Coupling length

In future optical communications systems, due to achieving high-integration density, it is essential to develop the ultra-compact photonic devices and subsystems. However, photonic subsystems with a high integration density are restricted by the cross talk between the adjacent waveguides, as well as the parameter of coupling length. It is defined as $L_c = \pi/(n_s - n_{as})$, where n_s and n_{as} are the real part of the mode effective refractive index of the symmetric and anti-symmetric modeof the two adjacent waveguides respectively[29].

Figure 6 shows the calculated coupling length L_c as a function of separation distance W in g=10 nm and g=20 nm for the center of two parallel waveguides. In the simulation the parameters are set as t=100 nm, D=100 nm, h=50 nm and θ=120°. The coupling length increases almost exponentially for both cases as W increases. The calculated results show that the coupling length can reach 10^5. So high-density independent function photonic elements are more easily integrated for our proposed structure.

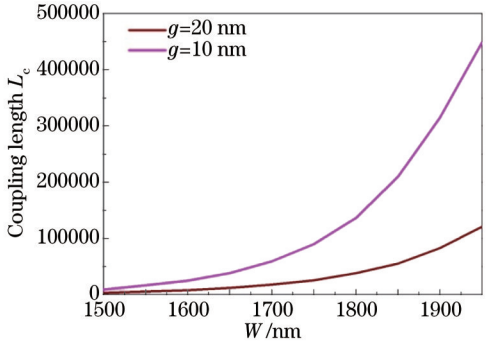

Fig.6 Coupling length L_c with W in different g (g=10 nm, g=20 nm)

4 Model properties versus curvature radius of wedge rounded tip

In practice, it is very difficult to fabricate an ideal sharp tip triangle wedge. Therefore, the fabricated nanowedges has a round tip. It is important therefore to investigate the influence of the radius of curvature of the nanowedges tip on its model properties. The waveguide parameters used in the simulation are given as following: t=100 nm, D=100 nm, h=50 nm, g=20 nm and θ=90°. From Figure 7(a) and (b), the calculated results show that the propagation distance decreases monotonically, while the normalized mode area is shown to decrease at first and then increase as the radius of curvature increases from 0 to 30 nm and the minimum value is at 5 nm. The results also show that the normalized mode area increases by 73% when the tip curvature increases from 0 to 30 nm, while the propagation distance decreases by 8% compared to that

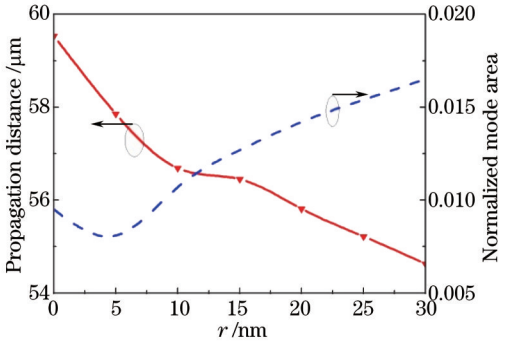

Fig.7 Propagation distance (solid lines) and the normalized mode area (dashed lines) with different radius of the rounded tip

for an ideal sharp tip.

5 MDM and DMD waveguide of the same structure

Finally, owing to quantitatively demonstrate the advantages of the proposed waveguide, it is compared with the DMD waveguide based on the same structure (the high index and metal region are exchange with each other). The parameters used in the simulations are t=100 nm, D=100 nm, h=50 nm, g=20 nm. Figure 8 (a) and (b) show the propagation distance and the normalized mode area separately. From figure 9, it shows that the proposed waveguide has better sub-wavelength mode confinement and low propagation loss than the DMD waveguide in the same tip angle. For example, at θ = 120°, the propagation distance of the proposed MDM waveguide is L_p = 59.96 μm , while L_p = 53.2 μm in the DMD waveguide. Meanwhile, the normalized mode area of the proposed MDM waveguide is A=0.013 as well as A=0.0345 of the DMD waveguide.

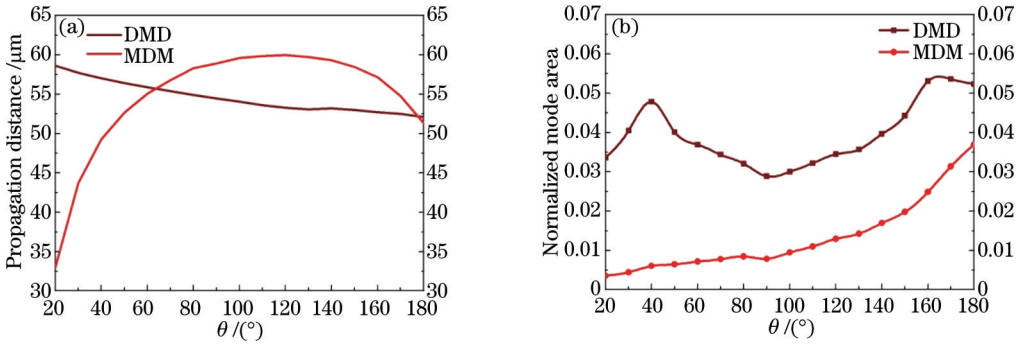

Fig.8 Contrast of the transmission characteristics of the DMD and MDM waveguides.
(a) Propagation distance; (b) normalized mode area

6 Conclusion

In summary, a MDM waveguide with the triangle wedge is proposed and numerically investigated. The model transmission characteristics have been discussed in the influence of the tip angle θ of the triangle nanowedges with the gap g. At 120°, it can achieve a trade-off relation between the propagation distance and the field confinement in the waveguide. Besides, by comparing with the DMD at the same structure and size, it shows ultra-deep-subwavelength light confinement with low loss. Meanwhile, the proposed structure also shows high tolerance for fabrication errors owing to a wide tip angle range. This proposed structure shows great potential in various applications, such as the laser, integrated circuits.

Reference

1 Krasavin A V, Zayats A V. Guiding light at the nanoscale: numerical optimization of ultrasubwavelength metallic wire plasmonic waveguides[J]. Opt Lett, 2011, 36(16): 3127-3129.

2 Ozbay E. Plasmonics: Merging photonics and electronics at nanoscale dimensions[J]. Science, 2006, 311(5758): 189-193.

3 Pohl M, Belotelow V I, Akimov I A. Plasmonic crystals for ultrafastnanophotonics: Optical switching of surface plasmonpolaritons[J]. Physical Review B, 2008, 85(8): 081401.

4 Zayats A V, Smolyaninov II, Maradudin A A. Maradudinc, Nano-optics of surface plasmonpolaritons[J]. Physics Reports, 2005, 408(3-4): 131-314.

5 Hu Qing, Xu Dihu, Zhou Yu, *et al*.. Position-sensitive spectral splitting with a plasmonic nanowire on silicon chip[J]. Scientific Reports, 2013, 3: 3095.

6 Wei Wei, Zhang Xia, Yu Hui, *et al*.. Plasmonic waveguiding properties of the gap plasmonmode with a dielectric substrate[J]. Photonics and Nanostructures-Fundamentals and Applications, 2013, 3(11): 279-287.

7 Ditlbacher H, Krenn J R, Schider G, *et al*.. Two-dimensional optics with surface plasmonpolaritons[J]. Applied Physics Letters, 2002, 81(10): 1762-1764.

8 Lin Chen, Tian Zhang, Xun Li. Novel hybrid plasmonic waveguide consisting of two identical dielectric nanowires

symmetrically placed on each side of a thin metal film[J]. Opt Express, 2012, 20(18): 20535-20544.

9 Li Xiaoer, Jiang Tao, Shen Linfang, *et al*.. Subwavelength guiding of channel plasmonpolaritons bytexturedmetallic grooves at telecom wavelengths[J]. Applied Physics Letters, 2013, 102(3): 031606.

10 Bian Yusheng, Zheng Zheng, Zhao Xin, *et al*.. Highly confined hybrid plasmonic modes guided by nanowire-embedded-metal grooves for low-loss propagation at 1550 nm[J]. IEEE Journal of Selected Topics in Quantum Electronics, 2013, 19(3): 4800106.

11 Lu Qijing, Chen Daru, Wu Genzhu. Low-loss hybrid plasmonic waveguide based on metal ridge and semiconductor nanowire[J]. Optics Communications, 2013, 289: 64-68.

12 Gosciniak J, Holmgaard T, Sergey I. Theoretical analysis of long-range dielectric-loaded surface plasmonpolariton waveguides[J]. Journal of Lightwave Technology, 2011, 29(10): 1473-1481.

13 Chen Lin, Li Xun, Gao Dingshan. An efficient directional coupling from dielectric waveguide to hybrid long-range plasmonic waveguide on a silicon platform[J]. Applied Physics B, 2013, 111: 15-19.

14 Zhang Guanmao, Sun Haili, Li Jianming. Study on the transmission characteristics of symmetric hybrid long-range surface plasmon polariton waveguide[J]. Laser & Optoelectronics Progress, 2013, 50(12): 121301.
张冠茂, 孙海丽, 李建明. 一种对称混合长程表面等离子激元波导传输特性研究[J]. 激光与光电子学进展, 2013, 50(12): 121301.

15 Chen Lin, Li Xun, Wang Guoping. A hybrid long-range plasmonic waveguide with sub-wavelength confinement[J]. Optics Communications, 2013, 291: 400-404.

16 Dong Qiming, Guo Xiaowei. Numerical analysis of SPP maskless interference lithography system[J]. Acta Photonica Sinica, 2012, 41(5): 558-564.
董启明, 郭小伟. 表面等离子体无掩膜干涉光刻系统的数值分析[J]. 光子学报, 2012, 41(5): 558-564.

17 Li Zhiquan, Gao Xiaoguang, Niu Liyong, *et al*.. Propagation properties of a surface plasmon polariton directional coupler [J]. Chinese J Lasers, 2012, 39(10): 1010001.
李志全, 高晓光, 牛力勇, 等. 一种表面等离子体激元定向耦合器的传输特性[J]. 中国激光, 2012, 39(10): 1010001.

18 Wu Pinghui, Gu Juguan, Liu Bin, *et al*.. Experimental research on wavelength modulation surface plasmon resonance sersor[J]. Laser & Optoelectronics Progress, 2012, 49(2): 022501.
吴平辉, 顾菊观, 刘 彬, 等. 波长检测型表面等离子体共振传感器的实验研究[J]. 激光与光电子学进展, 2012, 49(2): 022501.

19 Keshmarzi E K, Tait R N, Berini P. Long-range surface plasmon single-mode laser concepts[J]. Jounal of Applied Physics, 2012, 112(6): 063115.

20 Luo Daobin. The fluorescence rate of a single molecule close to a spherical metallic Nanoparticle[J]. Optik, 2014, 125 (16): 4352-4356.

21 Dai Daoxin, Shi Yaocheng, He Sailing. Gain enhancement in a hybrid plasmonicnano-waveguide with a low-index or high-index gain medium[J]. Opt Express, 2011, 19(14): 12925-12926.

22 Palik E D. Handbook of Optical Constants of Solids[M]. Boston: Academic Press, 1985.

23 Aspnes D E, Theeten J B. Spectroscopic analysis of the interface between SI and its thermally grown oxide[J]. Journal of the Electrochemical Society, 1979, 127(6): 1359-1365.

24 Adachi S. The Handbook on Optical Constants of Metals[M]. Singapore: World Scientific, 2012.

25 Sun Shulin, Chen HungTing, Zheng Weijin. Dispersion relation propagation length and mode conversion of surface plasmonpolaritons in silver double-nanowire systems[J]. Opt Express, 2013, 21(12): 14591-14605.

26 Oulton R F, Bartal G, Pile DFP. Confinement and propagation characteristics of subwavelength plasmonic modes[J]. New Journal of Physics, 2008, 10: 105018.

27 Tanaka K, Tanaka M, Katayama K, *et al*.. Propagation constants of guided waves in surface plasmonpolariton gap waveguides excited through an I-shaped aperture[J]. Comptes Rendus Physique, 2008, 9(1): 16-23.

28 Berini P. Figures of merit for surface plasmon waveguides[J]. Opt Express, 2006, 14(26): 13030-13042.

29 Ma Youqiao, Farrell G, Semenova Y, *et al*.. Novel dielectric-loaded plasmonic waveguide for tight-confined hybrid plasmonmode[J]. Plasmonic, 2013, 8(2): 1259-1263.

栏目编辑：韩 峰